Hilbert Transform and Statistical Analysis for Channel Selection and Epileptic Seizure Prediction

Heba M. Emara[1] · Mohamed Elwekeil[1] · Taha E. Taha[1] · Adel S. El-Fishawy[1] · El-Sayed M. El-Rabaie[1] · Turky Alotaiby[2] · Saleh A. Alshebeili[3] · Fathi E. Abd El-Samie[1,4]

Abstract

This paper is concerned with Electroencephalography (EEG) seizure prediction, which means the detection of the pre-ictal state prior to ictal activity occurrence. The basic idea of the proposed approach for EEG seizure prediction is to work on the signals in the Hilbert domain. The operation in the Hilbert domain guarantees working on the low-pass spectra of EEG signal segments to avoid artifacts. Signal attributes in the Hilbert domain including amplitude, derivative, local mean, local variance, and median are analyzed statistically to perform the channel selection and seizure prediction tasks. Pre-defined prediction and false-alarm probabilities are set to select the channels, the attributes, and bins of probability density functions (PDFs) that can be useful for seizure prediction. Due to the multi-channel nature of this process, there is a need for a majority voting strategy to take a decision for each signal segment. Simulation results reveal an average prediction rate of 96.46%, an average false-alarm rate of 0.028077/h and an average prediction time of 60.1595 min for a 90-min prediction horizon.

Keywords Epilepsy · EEG · Seizure prediction · Channel selection · Hilbert transform

1 Introduction

One of the most popular neurological diseases is epilepsy. It is widespread all over the world with about 1% of world population injured with this disease [1]. There is a need for certain precautions to deal with epilepsy patients to reduce the hazards facing them during seizure periods. That is why seizure prediction is necessary. If a seizure is predicted prior to its occurrence, alarms can be given to the patients to save them from dangerous actions [2]. Seizure prediction in itself is the process of anticipating a seizure prior to occurrence with a suitably long time. This also means the detection of the pre-ictal states from EEG signal activities if they are assumed to exist [3, 4].

Electroencephalogram (EEG) signals reflect the brain activities during human actions. For patients, epilepsy seizures occur due to some electrical discharges in groups

✉ Heba M. Emara
    hebam9909@gmail.com

Extended author information available on the last page of the article

of cells [5]. These discharges are reflected in EEG signals, which are recorded with different electrodes. Hence, EEG signals are of multi-channel nature. So, we can say that channel selection for epilepsy activity detection and prediction is a must [6–8]. In addition, technological improvements in implantable devices for seizure control [3, 4] have led to tremendous improvements in the accuracy and sensitivity of epileptic seizure prediction [9–11].

Several algorithms have been presented for EEG seizure prediction. Zandi et al. [12, 13] presented an approach for seizure prediction based on computing zero-crossing rate in sEEG with different window intervals. For each interval, the distribution of the histogram is computed. Then, the obtained distribution is compared with two reference inter-ictal and pre-ictal distributions. This approach presented an average sensitivity of 88.34%, an average prediction time of 22.5 min and a false prediction rate of 0.155/h. Hung et al. [14] presented a seizure prediction algorithm based on chaotic features in the wavelet domain. Their approach achieved an average accuracy of 87% with an average prediction time of 27 min and a false-alarm rate of 0.24/h.

Shiang et al. [15] developed a seizure prediction algorithm based on computing different attributes, namely cross-correlation, non-linear independence, difference of Lyapunov exponents and phase locking in the wavelet domain. A sensitivity of 74% was obtained. Gadhoumi et al. used wavelet features extracted from iEEG signals for seizure prediction. The features used in this approach are the entropy and wavelet energy. This approach achieved an accuracy of 85% with a false-alarm rate equal to 0.35/h [16]. In addition, the empirical mode decomposition (EMD) has also been utilized for EEG seizure prediction. The main advantage of the EMD is the ability to decompose the signal in an additive manner to a group of envelopes. Features are extracted from the intrinsic modes in the EMD domain. A hybrid feature extraction method based on three intrinsic mode functions (IMFs) and the variance of the envelope (VOE) of the approximation has been used [17]. Moreover, some sort of dimensionality reduction with principal component analysis (PCA) has been used in [18, 19].

The zero-crossing rate (ZCR) of EEG signals in the wavelet domain has been exploited for EEG seizure prediction [20]. The reason for using the ZCR is that in epileptic activities, rapid changes occur in EEG signals. These changes are estimated based on the ZCR in the wavelet domain. A support vector machine (SVM) has been used for the classification purpose. This algorithm achieved an average accuracy equal to 94%. N. Ozdemir et al. [21] adopted a seizure prediction algorithm based on Hilbert-Huang transform (HHT) and Bayesian classification. The HHT is utilized for feature extraction. After that, a correlation-based feature selection (CFS) algorithm is used to select the best features. Then, classification by means of Bayesian networks is implemented. A sensitivity of 96.55% and a false positive rate of 0.21/h were obtained.

Aarabi and He [22] presented a seizure prediction model based on the estimation of the spectra of iEEG signals. First, the EEG signal is band-pass filtered to be in the band of 0.5–100 Hz, and then notch filtered at 50 Hz. Then, the data is split into independent training and testing sets, and both are segmented into 10-s non-overlapping segments. The power spectral densities of 10-s iEEG segments are computed using the Welch spectral estimation method [23], where the signal is divided into segments overlapped by 50%, and then the Hamming window and the Fourier transform are applied. After that, the power spectra are computed. The Bayesian inference method is used to estimate the parameters of the model. This method achieved average sensitivities of 87.07 and 92.6% for maximum seizure occurrence periods of 30 and 50 min, respectively.

Alotaiby et al. [24] introduced a seizure prediction algorithm based on common spatial patterns (CSPs) as feature extractors. A linear discriminant analysis classifier is used for the classification purpose. Their algorithm achieved an average prediction time equal to 89%. The false prediction rate is 0.39/h, with an average prediction time of 68.71 min.

Myers et al. [25] presented a seizure prediction algorithm that depends on phase/amplitude lock values (PLV/ALV) by calculating the difference of phase and amplitude between electrodes that are local and remote to the epilepsy center. Their method reported an average sensitivity of 77%, and an average false prediction rate of 0.17/h. Consul et al. [26] presented a seizure prediction algorithm using phase difference in Hilbert domain. Their algorithm achieved a sensitivity of 88.2% with a prediction latency between 51 s and 188 min.

Chu et al. [27] presented a seizure prediction algorithm depending on attractor state analysis of the macroscopic dynamics of the brain. A sensitivity of 86.6%, a false prediction rate of 0.367/h and an average prediction time of 45.3 min were obtained. Sedik et al. [28] introduced a statistical framework for seizure prediction based on the utilization of digital filters. A prediction rate equal to 96.2485%, a false-alarm rate of 0.10526/h and a prediction time of 66.6 min were obtained. This framework has been applied only on 4 patients from the CHB-MIT dataset.

Daoud et al. [29] introduced a patient-specific seizure prediction algorithm using deep learning. Raw EEG signals are used as the input to the model without any pre-processing. Four deep learning models have been used to extract the most differentiating features to enhance the classification performance. Their algorithm achieved an average accuracy of 99.6% and a false-alarm rate of 0.004/h. Yang et al. [30] presented an approach for seizure prediction depending on permutation entropy as a main feature. An SVM has been used for the classification purpose. This approach achieved an average sensitivity of 94% and a false prediction rate of 0.111/h

This paper introduces a patient-specific algorithm for EEG channel selection and seizure prediction from sEEG. Signal attributes in the Hilbert domain including amplitude, derivative, local mean, local variance, and median are analyzed statistically to perform the channel selection and seizure prediction tasks. Pre-defined prediction and false-alarm probabilities are set to select the channels, the attributes, and bins of PDFs that can be useful for seizure prediction. In the training phase, EEG signal segments of length 10 s are analyzed into non-overlapping segments and filtered using a band-pass finite impulse response (FIR) filter (3–100 Hz) to remove undesired artifacts. Then, the Hilbert transform is estimated for each segment to compute the instantaneous amplitude. Figure 1 shows the instantaneous amplitudes for normal and pre-ictal segments. The selected signal attributes are treated statistically to yield PDFs. Seizure prediction is tested in this paper over three horizons of 30, 60, and 90 min, which are within the ranges used by other authors [13, 25, 27].

Contributions of the proposed approach are the utilization of the Hilbert transform to calculate the instantaneous amplitude of the analytic signals without the need for domain change, in addition to the simplicity of hardware implementation. Moreover, we introduce an adaptive channel selection algorithm, which specifies the effective channels for prediction. Moreover, we use a threshold-based classifier to decrease the computational complexity. The results obtained using the proposed approach are compared to those of previously published methods.
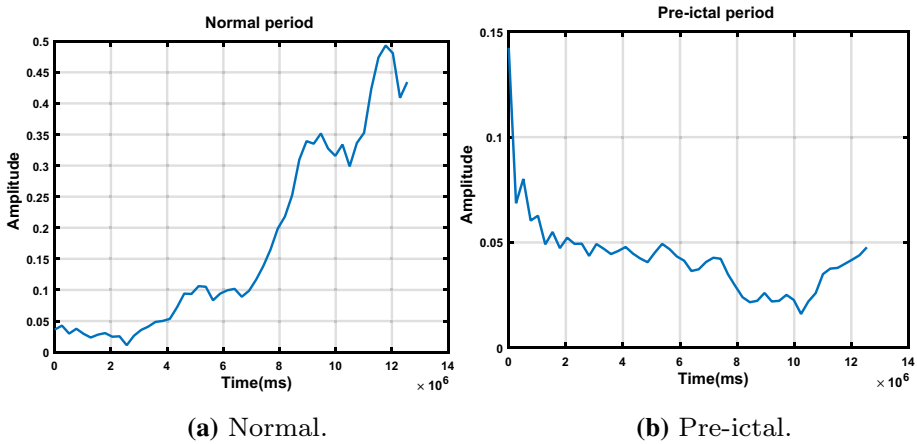
(a) Normal.

(b) Pre-ictal.

Fig. 1 Instantaneous amplitude in the Hilbert domain of normal and pre-ictal EEG segments

The rest of the paper is organized as follows. Section 2 provides materials and methods. Section 3 includes results and discussion. Finally, the conclusions are given in Sect. 4.

2 Materials and Methods

2.1 Dataset

Experiments are carried out on long-term continuous multi-channel scalp EEG recordings for 24 patients from the publicly available CHB-MIT dataset [31]. This dataset has been collected for 23 cases. One of them was recorded again after 1.5 years. All signals were measured with a sampling frequency of 256 Hz. The dataset for every patient has 23 channels, except for patients 12, 13, 14, 16, 17, 20, 21 and 22, who have 28 channels and patient 15, who has 31 channels. The dataset includes 686 sEEG hours. Table 1 introduces the seizure information for each case.

2.2 Hilbert Transform

Hilbert transform is a convolution between the Hilbert transformer $1/(\pi t)$ and the signal. It does not involve a change of domain, unlike many other transforms. The Hilbert transform of a signal $X(t)$ is calculated as follows [32]:

$$Y(t) = \frac{1}{\pi}P\int_{-\infty}^{\infty}\frac{X(\tau)}{t-\tau}d\tau \tag{1}$$

where P represents the Cauchy principal value of the integral. An analytic complex-time signal $Z(t)$ is constructed from a real-valued input signal $X(t)$ and the imaginary part $Y(t)$. The imaginary part represents the Hilbert transform of the real part. $A(t)$ is the instantaneous amplitude of the complex signal, and $\theta(t)$ is the phase of that signal.

Table 1 Seizure information for each case

Patient No.	No. of hours	No. of seizures	Gender	Age
1	40.55	7	F	11
2	35.16	3	M	11
3	36	7	F	14
4	150.7	4	M	22
5	39	5	F	7
6	68.24	10	F	1.5
7	67.05	3	F	14.5
8	20	5	M	3.5
9	65.02	4	F	10
10	50.02	7	M	3
11	34.62	3	F	12
12	23.671	40	F	2
13	32	12	F	3
14	25.851	8	F	9
15	39.42	20	M	16
16	19	10	F	7
17	22	3	F	12
18	35.633	6	F	18
19	29.93	3	F	19
20	27.595	8	F	6
21	31.816	4	F	13
22	32	3	F	9
23	25.733	7	F	6
24	12	16	M	12.5

$$Z(t) = X(t) + jY(t) = A(t)e^{j(\theta(t))} \tag{2}$$

$$A(t) = |Z(t)| \tag{3}$$

2.3 Statistical Analysis

Features extracted from the signals can be utilized to distinguish between normal and pre-ictal EEG states. The five statistical parameters representing the features used in the proposal are presented.

2.3.1 Signal Amplitude

The instantaneous amplitude after Hilbert transform is considered.

2.3.2 Signal Derivative

It is important to use a differentiator as a digital filter to acquire any abrupt changes in the signal. A suitable digital filter for this task is given by [33]:

$$H(z) = 1 - z^{-1} \tag{4}$$

2.3.3 Local Mean

Local mean is a measure of the signal trend. It can be estimated with a moving average filter of window $(2k + 1)$ as follows [34]:

$$\hat{X}(n) = \frac{1}{2k + 1} \sum_{m=n-k}^{n+k} X(m) \tag{5}$$

2.3.4 Local Variance

Local variance reflects how the signal is spread around the local mean. A moving average filter can be used for this task as follows [34]:

$$\hat{\sigma}_x^2(n) = \frac{1}{2k + 1} \sum_{m=n-k}^{n+k} (X(m) - \hat{X}(n))^2 \tag{6}$$

where $\hat{X}(n)$ represents the local mean of $X(n)$, which can be calculated using Eq. (5).

2.3.5 Instantaneous Median

Median filter is a type of order statistics filters. It depends on the selection of the median value of a certain signal segment as a tool to eliminate extrema of the signal. It can be implemented in a recursive or non-recursive manner. The non-recursive median filter output is given as [35]:

$$Y(n) = MED[X(n - k), \dots, X(n), \dots, X(n + k)] \tag{7}$$

where $X(n)$ and $Y(n)$ are the nth samples of the input and output sequences, respectively.

2.4 Statistical Analysis for EEG Signal Classification

The strategy adopted in the proposed approach is a thresholding strategy applied on certain bins extracted from certain PDFs. These bins must satisfy the distinguishability criteria between pre-ictal and normal states. The selection of bins and thresholds depends on setting pre-defined prediction and false-alarm probabilities. In our work in this paper, we set a prediction probability threshold of 70% and a false-alarm threshold of 30%. Firstly, known normal and pre-ictal signal segments of length 10 s are analyzed in
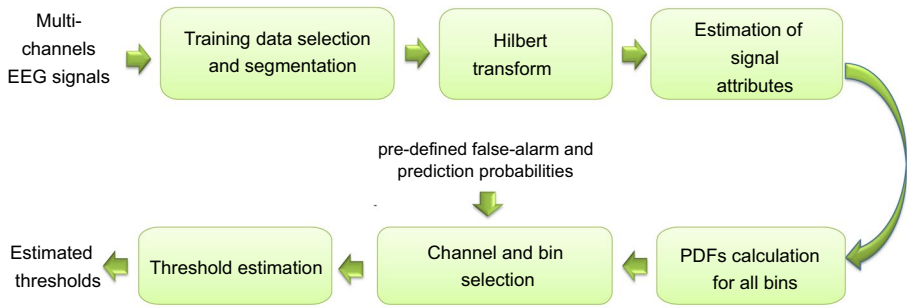
Fig. 2 Block diagram of the training phase of the proposed Hilbert-transform-based approach
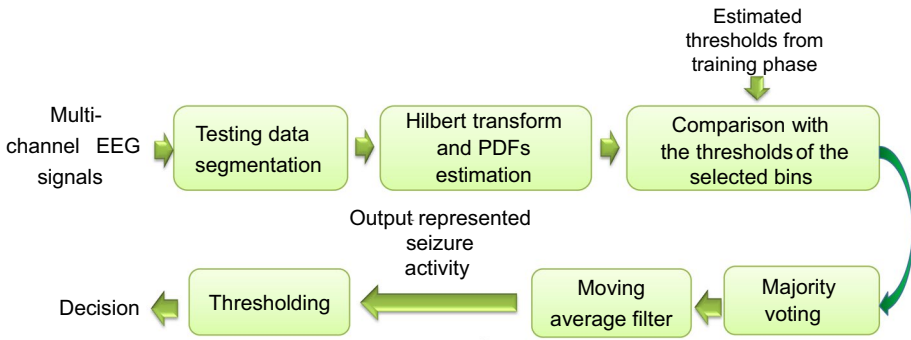
Fig. 3 Block diagram of the testing phase of the proposed Hilbert-transform-based approach

Hilbert domain. The selected signal attributes are treated statistically to yield PDFs for each attribute with 9 bins. Each bin is treated across signal segments as a random variable and the PDFs of these random variables are estimated to select the bins that satisfy the 70% for prediction probability and 30% for false-alarm probability for discrimination between normal and pre-ictal states. The intersection points between the PDFs of selected bins are estimated to determine the thresholds. Multiple decisions are taken for each incoming signal segment to decide whether it belongs to a normal or a pre-ictal activity. These decisions are merged together to yield a final decision about each segment. The training and testing phases are illustrated in Figs. 2 and 3, respectively.

2.4.1 Performance Metrics

Different evaluation metrics have been considered for the EEG seizure prediction process [8]:
The prediction rate (R_p) is calculated as:

$$R_p = \frac{N_p}{N_t} \tag{8}$$

The false-alarm rate (R_{fa}) is calculated as:

$$R_{fa} = \frac{N_{fa}}{H_t} \qquad (9)$$

The average prediction time (T_{avg}) is calculated as:

$$T_{avg} = \frac{T_p}{N_p} \qquad (10)$$

where N_p represents the number of predicted seizures, N_t is the total number of seizures, N_{fa} represents the number of false alarms, H_t is the total number of hours and T_p represents the prediction time.

3 Experimental Results and Discussion

For each segment of the EGG signal, five PDFs are estimated for each channel. These include amplitude, derivative, local mean, local variance, and median PDFs. Bin selection process for discrimination is performed on all bins from all PDFs from all channels. The prediction matrix in (11) reveals the bin selection and thresholding processes for patient 20. The first column determines the type of the attribute used for discrimination. (1) refers to amplitude, (2) refers to derivative, (3) refers to local mean, (4) refers to local variance and (5) refers to median. The second column determines the index of the selected channel. The third column determines the index of the bin selected for discrimination between normal and pre-ictal states.

We adopted 9 bins in each PDF. Prior to the prediction process, we set pre-defined prediction and false-alarm probability thresholds of 70% and 30%, respectively. Hence, the bins that satisfy the 70% predict probability with a false-alarm probability below 30% are selected. Hence, all values of column 4 are larger than 70%, and all values of column 5 are below 30%. Each selected bin is treated as a random number across segments. Hence, the PDF of the selected bin itself differs between pre-ictal and normal states. Two different distributions for both states intersect with a certain threshold chosen for discrimination as shown in Fig. 4. The threshold differs for each selected bin. Hence, different values of the thresholds lie in column 6. To discriminate between two scenarios, we put 1 or 0 for each state of the normal distribution on the right or on the left as shown in column 7.
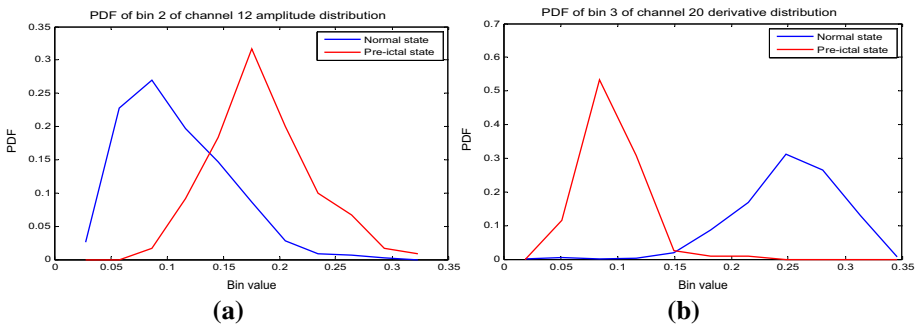
Fig. 4 PDFs for amplitude and derivative attributes

Fig. 5 Majority voting results for patient 1
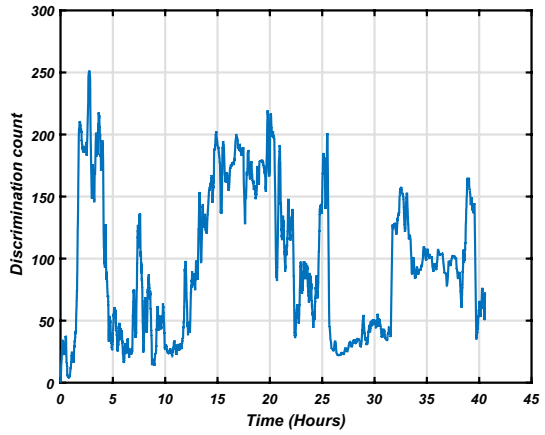
Fig. 6 Majority voting results for patient 8
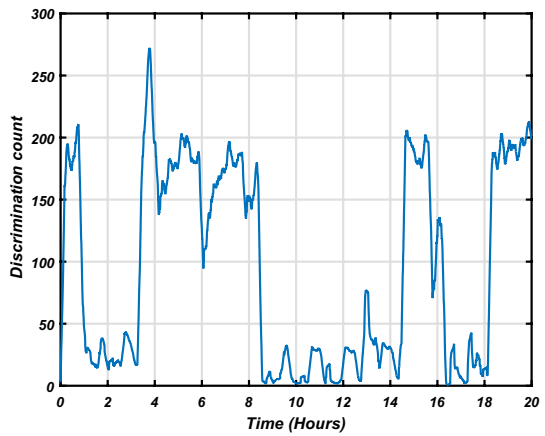
Fig. 7 Majority voting results for patient 14
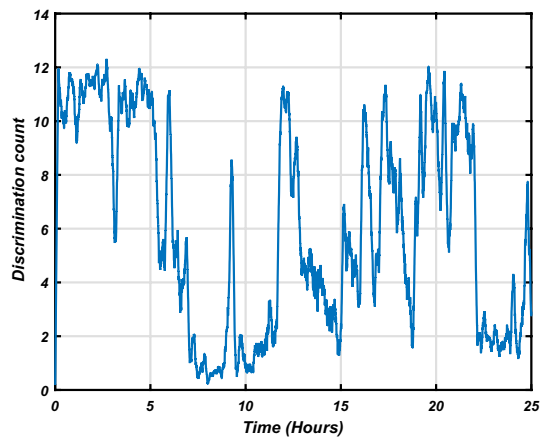
Fig. 8 Majority voting results for patient 20
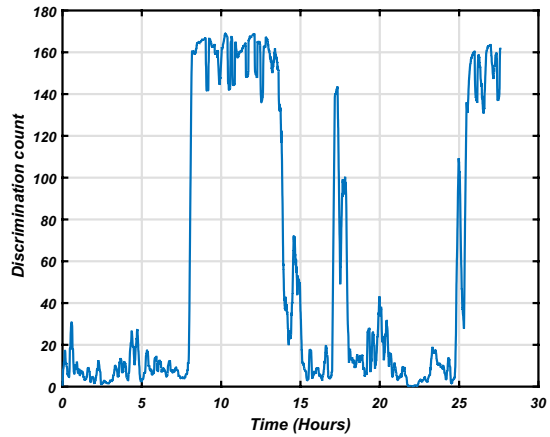
A group of decisions is obtained for each segment. Some of them are positive, meaning a pre-ictal state, and some are negative meaning a normal state. If we represent the positive decisions with 1 and the negative decisions with 0, an averaging or majority voting process gives a certain indicator from the state. The obtained signal needs some smoothing with a non-recursive averaging filter. A filter of such type with length 60 is used to get a discrete time sequence representing the segment diagnosis state. In this paper, we adopt the name of discrimination count for this sequence. The level-crossing strategy is applied on this count for seizure prediction. Figures 5, 6, 7 and 8 show the majority voting results for patients 1, 8, 14 and 20, respectively. The horizontal axis represents the selected segment index and the vertical axis represents the bins that are selected for classification.

Different prediction horizons of 30, 60 and 90 min have been considered in our simulation experiments. The prediction horizon represents the period within which a seizure is anticipated. A long prediction horizon is preferred due to the ability to predict seizures as early as possible, which allows an alert to be sent to the patient or the care-giver very early to take an action to save the patient's life. A 15-min post-seizure horizon is taken into consideration. In this horizon, all prediction alerts are ignored. The prediction time (T_P) in our simulations is the time between the prediction alert and the start of the ictal state.

$$P = \begin{pmatrix} 2 & 2 & 2 & 0.95000 & 0.079167 & 0.072266 & 1 \\ 5 & 12 & 2 & 0.7083 & 0.2806 & 0.1599 & 1 \\ 2 & 3 & 2 & 0.95000 & 0.084722 & 0.073398 & 1 \\ 3 & 12 & 9 & 0.7000 & 0.2667 & 0.1587 & 1 \\ \vdots & \vdots & \vdots & \vdots & \vdots & \vdots & \vdots \\ 1 & 20 & 4 & 0.7083 & 0.2792 & 0.1606 & 0 \\ 4 & 4 & 5 & 1.0000 & 0.075 & 0.204102 & 1 \\ 2 & 20 & 6 & 0.941667 & 0.1875 & 0.023281 & 1 \\ 4 & 3 & 7 & 0.916667 & 0.118056 & 0.011953 & 0 \end{pmatrix} \tag{11}$$

Table 2 Evaluation parameters

Patient No.	Pred. prob. constraint (%)	False-alarm prob. constraint (%)	Time domain D_{th}	FFT D_{th}	WT D_{th}	HT D_{th}
1	70	30	140	120	120	140
2	70	30	5	50	43	60
3	60	40	8	10	13	15
4	60	40	25	15	12	10
5	70	30	15	15	10	12
6	70	30	25	12	12	7
7	70	30	35	23	20	17
8	70	30	150	120	140	170
9	70	30	120	140	150	100
10	70	30	70	50	80	75
11	70	30	2	5	4	7
12	70	30	20	15	13	15
13	60	40	45	60	35	50
14	60	40	70	70	60	65
15	70	30	50	37	45	30
16	70	30	120	150	135	150
17	60	40	5	15	12	10
18	70	30	60	45	55	62
19	70	30	2	1.5	3	4
20	70	30	120	130	120	150
21	60	40	7	10	12	5
22	60	40	4	3.5	5	4
23	70	30	40	42	45	37
24	70	30	3.5	2	2.5	3.5

Table 2 presents the evaluation parameters, where the first and second columns show the prediction probability constraint and the false-alarm probability constraint, respectively. The third, fourth, fifth and sixth columns represent the decision threshold (D_{th}) for each patient from the dataset for time domain, fast Fourier transform (FFT), wavelet transform (WT) and the proposed approach using the Hilbert transform (HT), respectively.

In order to study the impact of the transform on the performance of the proposed approach, a comparison between the time-domain, frequency-domain, wavelet-domain and the proposed HT-based approach for 30, 60 and 90 min horizons is presented.

3.1 Results for 30-min Horizon

The results for 30-min horizon are presented in Table 3. It is clear that the proposed approach outperforms the time-domain, frequency-domain and wavelet-domain approaches in terms of prediction time T_P, number of false alarms N_{FA} and number of predicted seizures N_P.

For example, for patient 1, although the proposed approach has the same prediction rate as those of both the time-domain and the wavelet-domain approaches, it has better

Table 3 Performance comparison between all approaches for the 30-min horizon

Patient No.	No. of seizures	Time-domain approach			Frequency-domain approach			Wavelet-domain approach			Proposed approach		
		N_p	N_{fa}	T_p (min)	N_p	N_{fa}	T_p (min)	N_p	N_{fa}	T_p (min)	N_p	N_{fa}	T_p (min)
1	7	6	8	22.52	4	9	29.43	6	6	15.66	6	3	26
2	3	2	10	23.24	2	9	30	3	22	20	2	6	23.58
3	7	5	9	20.58	6	12	27.18	5	14	19.95	7	0	24.51
4	4	3	6	19.69	4	5	21.28	4	3	20.21	4	3	28.57
5	5	4	10	25.8	5	15	30	4	7	30	4	4	24.9
6	10	7	16	23.15	8	15	26.55	7	5	20.39	9	4	29.4
7	3	2	12	26.9	2	10	30	2	8	30	3	6	29.8
8	5	5	3	24.25	5	1	27.79	5	4	28.15	5	1	29
9	4	2	3	17.87	3	3	16.53	3	6	20.43	3	3	23.78
10	7	4	9	15.54	5	10	20.17	6	8	22.13	6	4	21.34
11	3	2	3	16.05	2	3	19.2	2	4	15.23	2	2	19.51
12	40	35	10	11.56	36	8	10.17	37	7	16.73	38	2	15.12
13	12	10	4	20.98	11	5	23.16	11	6	20.19	11	2	22.76
14	8	7	6	25	6	7	17.7	6	6	18.13	7	6	22.9
15	20	18	5	15.23	18	3	18.19	18	4	17.67	20	1	20.84
16	10	7	8	25	8	6	23.13	8	5	25	8	2	19.76
17	3	2	6	20.64	2	4	21.23	2	6	22	2	4	27.79
18	6	4	7	23.45	5	11	20.42	4	5	19.78	5	3	22.86
19	3	2	8	21.06	2	10	20.68	2	8	26.89	2	5	30
20	8	8	2	21.26	8	7	24.5	6	2	25.1	8	1	23.12
21	4	2	10	23.15	3	12	20.54	4	19	28.03	3	5	27.73
22	3	2	10	22.46	2	8	24.45	2	13	30	2	6	28.9
23	7	5	8	20	5	6	21.34	5	9	23.45	6	1	25.06
24	16	13	5	20.67	14	2	18.34	5	3	25.56	15	0	29.54
Total	198	130	178	459.28	166	172	370.46	167	180	512.53	178	74	541.77

Table 3 (continued)

Patient No.	No. of seizures	Time-domain approach			Frequency-domain approach			Wavelet-domain approach			Proposed approach		
		N_p	N_{fa}	T_p (min)	N_p	N_{fa}	T_p (min)	N_p	N_{fa}	T_p (min)	N_p	N_{fa}	T_p (min)
R_p (%)		65.65			83.8			84.34			89.9		
R_{fa} (/h)		0.1851			0.1788			0.1871			0.077		
Average T_p (min)		19.14			15.44			21.36			22.57		

performance in terms of false-alarm rate and prediction time compared to these approaches. Moreover, the frequency-domain approach achieves a longer prediction time compared to the proposed approach by about 4 min. In addition, the proposed approach reduces the false-alarm rate by about 66.67% of that of the frequency-domain approach. Furthermore, the proposed approach increases the number of predicted seizures by about 50% of that of the frequency-domain approach.

In addition, let us concentrate on the results of patient 15, where the proposed approach provides a 100% prediction rate. Furthermore, it provides a prediction time, which is longer than those of the time-domain, frequency-domain and wavelet-domain approaches by values that are about 5.61, 3, and 3 min, respectively. Moreover, the proposed approach reduces the false-alarm rate by about 80, 66.67, and 75% compared to those of the time-domain, frequency-domain and wavelet-domain approaches, respectively.

The prediction rate is estimated based on the number of predicted seizures. The prediction of a seizure depends on the detection of a single alert prior to the seizure within the prediction horizon. The proposed approach provides an average prediction rate of 89.9% for all patients. It improves the average prediction rate for all patients by values that reach 37, 7.3, and 6.6% compared to those of the time-domain, frequency-domain and wavelet-domain approaches, respectively. Moreover, the proposed approach reduces the false-alarm rate for all patients by about 58.4, 56.9, and 58.84% compared to those of the time-domain, frequency-domain and wavelet-domain approaches, respectively.

3.2 Results for 60-min Horizon

The obtained results for 60-min horizon are given in Table 4. It is clear from the results that the proposed approach improves the prediction rate by values that reach 9.76, 3.45, and 4.65% compared to those of the time-domain, frequency-domain and wavelet-domain approaches, respectively. It is noteworthy that the proposed approach produces a 100% prediction rate for patients 3, 4, 7, 8, 11, 15, 18, and 20. Moreover, the proposed approach reduces the false-alarm rate for all patients by about 61.1, 67.7, and 62.5% compared to those of the time-domain, frequency-domain and wavelet-domain approaches, respectively. It should be noted that the proposed approach produces zero false alarms for patients 3, 11, and 24.

Furthermore, the proposed approach provides an average prediction time for all patients, which is longer than those of the time-domain, frequency-domain and wavelet-domain approaches by values that are about 13.6, 8.83, and 17.1 min, respectively. This means that the proposed approach can predict the seizures earlier than rival approaches, and hence it allows the patients to take the necessary precautions earlier before the occurrence of the seizure. For example, for patient 9, the proposed approach provides a prediction time that reaches 56.78 min, which is longer than those of the time-domain, frequency-domain and wavelet-domain approaches by values that are about 21.19, 23.92, and 23.34 min, respectively.

Considering another patient, specifically patient 19, it is clear that the proposed approach provides a prediction time that reaches 56.85 min, which is longer than those of the time-domain, frequency-domain and wavelet-domain approaches by values that are about 13, 7.6, and 17.16 min, respectively.

Table 4 Performance comparison between all approaches for the 60-min horizon

Patient No.	No. of seizures	Time-domain approach			Frequency-domain approach			Wavelet-domain approach			Proposed approach		
		N_p	N_{fa}	T_p (min)	N_p	N_{fa}	T_p (min)	N_p	N_{fa}	T_p (min)	N_p	N_{fa}	T_p (min)
1	7	6	4	37.9	5	8	42.86	6	6	25.66	6	2	46.68
2	3	2	7	33.54	2	9	43.18	3	18	33.56	2	2	40.56
3	7	5	5	42.67	6	12	43.05	5	14	37.72	7	0	42.62
4	4	3	3	41.73	4	5	35.36	4	2	40.78	4	2	45.34
5	5	4	7	45.69	5	13	52.19	4	7	57.69	4	3	40.03
6	10	7	12	43.74	8	13	52.34	7	5	38.39	9	4	53.56
7	3	2	11	50.88	2	10	50.58	2	8	38.12	3	5	49.89
8	5	5	2	46.13	5	1	46.03	5	4	40.15	5	1	44.15
9	4	2	3	35.62	3	3	32.86	3	4	33.44	3	3	56.78
10	7	5	6	43.83	6	8	42.56	6	5	45.67	6	3	53.13
11	3	2	3	38.36	3	4	40.23	2	3	40.55	3	0	45.78
12	40	37	7	28.56	37	5	30.27	37	5	29.18	38	2	33.34
13	12	11	4	46.63	11	5	52.51	11	5	50.45	11	2	57.14
14	8	7	4	30.4	6	7	19.7	7	4	32.77	7	5	**33.65**
15	20	19	3	49.89	19	2	48.17	19	3	45.34	20	1	45.89
16	10	7	5	40.67	8	6	45.36	8	5	45.03	8	2	42.61
17	3	2	6	44.32	2	3	45.26	2	2	42.47	2	1	50.72
18	6	5	6	47.12	6	8	40.31	5	3	43.49	6	2	50.44
19	3	2	8	43.87	2	7	49.27		6	39.69	2	3	56.85
20	8	8	1	29.57	8	7	34.98	8	0	37.67	8	1	35
21	4	2	10	40.55	3	11	43.91	4	10	32.57	3	2	48.66
22	3	2	6	43.06	2	5	47.69	2	8	45.89	2	4	47.88
23	7	5	5	39.79	6	4	51.31	5	6	37.75	6	1	53.61
24	16	14	3	42.67	15	2	40.46	15	3	43.67	15	0	47.12
Total	198	164	131	987.17	174	158	1030.44	172	136	957.7	180	51	1121.43

Table 4 (continued)

Patient No.	No. of seizures	Time-domain approach			Frequency-domain approach			Wavelet-domain approach			Proposed approach		
		N_p	N_{fa}	T_p (min)	N_p	N_{fa}	T_p (min)	N_p	N_{fa}	T_p (min)	N_p	N_{fa}	T_p (min)
R_p (%)		82.8			87.9			86.88			90.9		
R_{fa} (/h)		0.136226			0.164303			0.141425			0.053034		
Average T_p (min)		41.13208			42.935			39.90417			46.72625		

Table 5 Performance comparison between all approaches for 90-min horizon

Patient No.	No. of seizures	Time-domain approach			Frequency-domain approach			Wavelet-domain approach			Proposed approach		
		N_p	N_{fa}	T_p (min)	N_p	N_{fa}	T_p (min)	N_p	N_{fa}	T_p (min)	N_p	N_{fa}	T_p (min)
1	7	6	4	48.45	5	8	45.31	7	5	39.89	7	1	61.57
2	3	2	5	56.89	2	3	46.85	3	8	45.86	3	2	65.78
3	7	5	5	46.78	6	9	49.71	6	10	45.12	7	0	56.63
4	4	3	2	49.51	4	3	45.75	4	2	50.08	4	0	64.89
5	5	4	6	49.91	5	10	60.77	4	5	61.03	5	1	54.77
6	10	8	10	47.32	5	13	59.13	4	5	48.88	9	1	65.12
7	3	2	8	55.67	2	6	57.85	2	5	49.13	3	2	57.88
8	5	5	1	46.13	5	1	56.23	5	4	43.56	5	1	47.95
9	4	2	3	43.47	3	3	45.78	3	4	46.89	3	3	66.81
10	7	5	6	49.85	6	6	50.89	6	3	54.34	7	3	60.72
11	3	2	3	61.78	3	2	64.62	3	2	63.81	3	0	68.23
12	40	39	3	56.89	39	3	67.23	39	4	55.6	40	0	70.88
13	12	11	4	56.7	11	4	56.89	11	4	62.67	11	1	67.13
14	8	7	2	45.76	7	5	56.87	7	3	54.98	7	3	53.07
15	20	19	2	57.47	19	2	57.8	19	1	58.9	20	1	67.3
16	10	7	3	45.3	8	4	55.6	8	2	56.76	8	0	59.78
17	3	2	3	49.77	2	3	50.8	2	2	56.8	2	1	64.22
18	6	5	3	47.12	6	5	58.46	5	1	55.95	6	1	66.02
19	3	2	6	48.67	2	4	56.34	2	5	47.87	2	2	71.9
20	8	8	0	35.76	8	5	36.98	8	0	40.77	8	0	38.15
21	4	2	7	45.33	3	5	47.25	3	5	47.87	3	2	52.7
22	3	2	3	45.6	2	4	47.69	2	5	48.71	2	1	51.22
23	7	5	3	42.76	6	3	55.7	5	3	45.7	6	1	56.3
24	16	14	2	48.9	15	2	45.71	15	3	47.8	15	0	54.8
Total	198	167	94	1181.79	174	113	1276.21	173	91	1228.97	191	27	1443.83

Table 5 (continued)

Patient No.	No. of seizures	Time-domain approach			Frequency-domain approach			Wavelet-domain approach			Proposed approach		
		N_p	N_{fa}	T_p (min)	N_p	N_{fa}	T_p (min)	N_p	N_{fa}	T_p (min)	N_p	N_{fa}	T_p (min)
R_p (%)		84.34			87.9			87.4			96.46		
R_{fa} (/h)		0.09775			0.117508			0.09463			0.028077		
Average T_p (min)		49.24125			53.17542			51.20708			60.15958		

Table 6 Comparison between the proposed approach and other published approaches

Author	Year	Patients	R_p (%)	R_{fa} (/h)	T_p (min)
Chiang et al. [15]	2011	7 patients from CHB-MIT 1 patient from NTUH	52.2	–	–
Zandi et al. [13]	2013	17 patients from VGH 3 patients from CHB-MIT	88.34	0.155	22.5
Consul et al. [26]	2013	10 patients from CHB-MIT	88.2	–	51 s–188 min
Myers et al. [25]	2016	10 patients from CHB-MIT	77	0.17	–
Chu et al. [27]	2017	13 patients from CHB-MIT 3 patients from SNUH	86.67	0.367	–
Alotaiby et al. [24]	2017	24 patients from CHB-MIT	87	0.4	52.7
Yang et al. [30]	2018	19 patients from Freiburg	94	0.111	61.93
Sediek et al. [28]	2019	4 patients from CHB-MIT	96.2485	0.10526	66.6
Proposed approach					
30-min horizon	–	24 patients from CHB-MIT	89.9	0.077	22.57
60-min horizon			90.9	0.053034	46.72625
90-min horizon			96.46	0.028077	60.15958

3.3 Results for 90-min Horizon

A summary of the results for the 90-min horizon is presented in Table 5. The proposed approach provides a 96.46% average prediction rate for all patients, which is higher than those of the time-domain, frequency-domain and wavelet-domain approaches by 14.4, 9.8, and 10.4%, respectively. Specifically, the proposed approach achieves a 100% prediction rate for patients 1, 2, 3, 4, 5, 7, 8, 10, 11, 12, 15, 18, and 20. In addition, the proposed approach produces an average prediction time for all patients, which reaches 60.15958 min. It is longer than those of the time-domain, frequency-domain and wavelet-domain approaches by values that are about 22.2, 13.1, and 17.5 min, respectively.

Moreover, the proposed approach has a better performance in terms of false-alarm rate. I reduces the false-alarm rate for all patients by about 71.3, 76.1, and 70.3% of those of the time-domain, frequency-domain and wavelet-domain approaches, respectively. Specifically, the proposed approach provides zero false alarms for patients 3, 4, 11, 12, 16, 20, and 24.

3.4 Comparison with Existing Seizure Prediction Approaches

The comparison of the proposed prediction approach with other published approaches is shown in Table 6. Improvements in performance in terms of prediction rate, false-alarm rate and prediction time are obtained with less computational complexity. In addition, an adaptive algorithm for channel selection and a simple thresholding-based classifier are used. The proposed approach provides prediction rates that are 45.88, 8.42, 8.56, 20.17, 10.15, and 9.8% higher than those of the approaches presented in [13, 15, 25–27] and [24], respectively. In addition, it reduces the false-alarm rate R_{fa} by 81.9, 83.5, 92.4, 93, 74, and 72% compared to those of [13, 25, 27, 24, 30] and [28], respectively. Moreover, it provides prediction times that are 62.62 and 14.23% higher than those of [13] and [24].

4 Conclusions

This paper presented an efficient seizure prediction approach that depends on statistical analysis of EEG signals in the Hilbert domain. The PDFs are estimated for signal attributes, and their bins are traced to select the most appropriate ones for seizure prediction under certain constraints. Seizure prediction has been tested in this paper over three horizons. Simulation results proved that the 90-min horizon is the best for efficient seizure prediction. In addition, the comparison with the published approaches for EEG seizure prediction ensures superiority of the proposed approach from the prediction time, prediction rate, and false-alarm rate perspectives.

References

1. WHO. (2017). *Programmes and projects*. http://www.who.int/mediacentre/factsheets/fs999/en/. Online; Accessed 20 May 2017.
2. Elger, C. E. (2001). Future trends in epileptology. *Current Opinion in Neurology*, *14*(2), 185–186.
3. Stacey, W. C., & Litt, B. (2008). Technology insight: Neuroengineering and epilepsy-designing devices for seizure control. *Nature Clinical Practice Neurology*, *4*(4), 190–201.
4. Cook, M. J., O'Brien, T. J., Berkovic, S. F., Murphy, M., Morokoff, A., Fabinyi, G., et al. (2013). Prediction of seizure likelihood with a long-term, implanted seizure advisory system in patients with drug-resistant epilepsy: A first-in-man study. *The Lancet Neurology*, *12*(6), 563–571.
5. Adeli, H., Zhou, Z., & Dadmehr, N. (2003). Analysis of EEG records in an epileptic patient using wavelet transform. *Journal of Neuroscience Methods*, *123*(1), 69–87.
6. Alotaiby, T., Abd El-Samie, F. E., Alshebeili, S. A., & Ahmad, I. (2015). A review of channel selection algorithms for EEG signal processing. *EURASIP Journal on Advances in Signal Processing*, *20*(1), 66.
7. Abd El-Samie, F. E., Alotaiby, T. N., Khalid, M. I., Alshebeili, S. A., & Aldosari, S. A. (2018). A review of EEG and meg epileptic spike detection algorithms. *IEEE Access*, *6*, 60,673–60,688.
8. Aarabi, A., Fazel-Rezai, R., & Aghakhani, Y. (2009). EEG seizure prediction: Measures and challenges. In *Annual international conference of the IEEE engineering in medicine and biology society, 2009. EMBC 2009* (pp. 1864–1867). IEEE.
9. Mormann, F., Kreuz, T., Rieke, C., Andrzejak, R. G., Kraskov, A., David, P., et al. (2005). On the predictability of epileptic seizures. *Clinical Neurophysiology*, *116*(3), 569–587.
10. Park, Y., Luo, L., Parhi, K. K., & Netoff, T. (2011). Seizure prediction with spectral power of EEG using cost-sensitive support vector machines. *Epilepsia*, *52*(10), 1761–1770.
11. Gardner, A. B., Krieger, A. M., Vachtsevanos, G., & Litt, B. (2006). One-class novelty detection for seizure analysis from intracranial EEG. *Journal of Machine Learning Research*, *7*, 1025–1044.
12. Zandi, A. S., Tafreshi, R., Javidan, M., & Dumont, G. A. (2010). Predicting temporal lobe epileptic seizures based on zero-crossing interval analysis in scalp EEG. In *2010 Annual international conference of the IEEE engineering in medicine and biology society (EMBC)* (pp. 5537–5540). IEEE.
13. Zandi, A. S., Tafreshi, R., Javidan, M., & Dumont, G. A. (2013). Predicting epileptic seizures in scalp EEG based on a variational Bayesian gaussian mixture model of zero-crossing intervals. *IEEE Transactions on Biomedical Engineering*, *60*(5), 1401–1413.
14. Hung, S.-H., Chao, C.-F., Wang, S.-K., Lin, B.-S., & Lin, C.-T. (2010). VLSI implementation for epileptic seizure prediction system based on wavelet and chaos theory. In *TENCON 2010–2010 IEEE region 10 conference* (pp. 364–368). IEEE.
15. Chiang, C.-Y., Chang, N.-F., Chen, T.-C., Chen, H.-H., & Chen, L.-G. (2011). Seizure prediction based on classification of EEG synchronization patterns with on-line retraining and post-processing scheme. In *2011 Annual international conference of the IEEE engineering in medicine and biology society, EMBC* (pp. 7564–7569). IEEE.
16. Gadhoumi, K., Lina, J.-M., & Gotman, J. (2013). Seizure prediction in patients with mesial temporal lobe epilepsy using EEG measures of state similarity. *Clinical Neurophysiology*, *124*(9), 1745–1754.

17. Qi, Y., Wang, Y., Zheng, X., Zhang, J., Zhu, J., & Guo, J. (2012). Efficient epileptic seizure detection by a combined IMF-VoE feature. In *2012 Annual international conference of the IEEE engineering in medicine and biology society (EMBC)* (pp. 5170–5173). IEEE.
18. Xie, S., & Krishnan, S. (2011). Signal decomposition by multi-scale PCA and its applications to long-term EEG signal classification. In *2011 IEEE/ICME international conference on complex medical engineering (CME)* (pp. 532–537). IEEE.
19. Williamson, J. R., Bliss, D. W., Browne, D. W., & Narayanan, J. T. (2012). Seizure prediction using EEG spatiotemporal correlation structure. *Epilepsy and Behavior*, *25*(2), 230–238.
20. Elgohary, S., Eldawlatly, S., & Khalil, M. I. (2016). Epileptic seizure prediction using zero-crossings analysis of EEG wavelet detail coefficients. In *2016 IEEE conference on computational intelligence in bioinformatics and computational biology (CIBCB)* (pp. 1–6). IEEE.
21. Ozdemir, N., & Yildirim, E. (2014). Patient specific seizure prediction system using Hilbert spectrum and Bayesian networks classifiers. In *Computational and mathematical methods in medicine* (Vol. 2014).
22. Aarabi, A., & He, B. (2014). Seizure prediction in hippocampal and neocortical epilepsy using a model-based approach. *Clinical Neurophysiology*, *125*(5), 930–940.
23. Welch, P. (1967). The use of fast Fourier transform for the estimation of power spectra: A method based on time averaging over short, modified periodograms. *IEEE Transactions on Audio and Electroacoustics*, *15*(2), 70–73.
24. Alotaiby, T. N., Alshebeili, S. A., Alotaibi, F. M., & Alrshoud, S. R. (2017). Epileptic seizure prediction using CSP and LDA for scalp EEG signals. In *Computational intelligence and neuroscience* (Vol. 2017).
25. Myers, M. H., Padmanabha, A., Hossain, G., de Jongh Curry, A. L., & Blaha, C. D. (2016). Seizure prediction and detection via phase and amplitude lock values. *Frontiers in Human Neuroscience*, *10*, 80.
26. Consul, S., Morshed, B. I., & Kozma, R. (2013). Hardware efficient seizure prediction algorithm. In *Nanosensors, biosensors, and info-tech sensors and systems 2013* (Vol. 8691, p. 86911J). International Society for Optics and Photonics.
27. Chu, H., Chung, C. K., Jeong, W., & Cho, K.-H. (2017). Predicting epileptic seizures from scalp EEG based on attractor state analysis. *Computer Methods and Programs in Biomedicine*, *143*, 75–87.
28. Sedik, A., Emara, H. M., Hamad, A., Shahin, E. M., El-Hag, N. A., Khalil, A., et al. (2019). Efficient anomaly detection from medical signals and images. *International Journal of Speech Technology*, *22*(3), 739–767.
29. Daoud, H., & Bayoumi, M. A. (2019). Efficient epileptic seizure prediction based on deep learning. *IEEE Transactions on Biomedical Circuits and Systems*, *13*(5), 804–813.
30. Yang, Y., Zhou, M., Niu, Y., Li, C., Cao, R., Wang, B., et al. (2018). Epileptic seizure prediction based on permutation entropy. *Frontiers in Computational Neuroscience*, *12*, 55.
31. PhysioNet. (2000). *CHB-MIT scalp EEG database*. https://www.physionet.org/pn6/chbmit/. Online; Accessed 1 January 2017.
32. Poularikas, A. D. (1998). *Handbook of formulas and tables for signal processing* (Vol. 13). Boca Raton: CRC Press.
33. Kuo, S. M., Lee, B. H., & Tian, W. (2013). *Real-time digital signal processing: Fundamentals, implementations and applications*. Chichester: Wiley.
34. El-Samie, F. E. A. (2011). Information security for automatic speaker identification. In *Information security for automatic speaker identification* (pp. 1–122). Springer.
35. Yin, L., Yang, R., Gabbouj, M., & Neuvo, Y. (1996). Weighted median filters: A tutorial. *IEEE Transactions on Circuits and Systems II: Analog and Digital Signal Processing*, *43*(3), 157–192.

Heba M. Emara received the B.Sc. and M.Sc. degrees from Menoufia University, Menouf, Egypt, in 2002, and 2019, respectively. Her current research interests include image processing, medical signal and image processing, and digital communications.

Mohamed Elwekeil received the B.Sc. in Electronics and Electrical Communications Engineering from the Faculty of Electronic Engineering, Menoufia University, Egypt in 2007. He received the M.Sc. and the Ph.D. degrees in Electronics and Communications Engineering from Egypt-Japan University of Science and Technology (E-JUST), Alexandria, Egypt in 2013 and 2016, respectively. He was a Teaching Assistant in the Department of Electronics and Electrical Communications Engineering, Faculty of Electronic Engineering, Menoufia University, Egypt in the period from December 2007 to November 2016. In December 2016, he has been promoted to a Lecturer (Assistant Professor) position in the same department. In the period from April 2014 till March 2015, he was a Research Intern at Alcatel-Lucent Bell N.V. (now NOKIA), Antwerp, Belgium, where he was working on WiFi optimization project. In October 2015, he has joined Kyushu University, Fukuoka, Japan, as a Special Research Student for a period of 9 months. In the period from April 2018 to March 2020, he was with the College of Information Engineering, Shenzhen University, Shenzhen, China, where he was working as a Post-Doctoral Researcher. His research interests include radio resource management for wireless networks, spatial modulation, and signal processing for communications.

Taha E. Tah was born in Tanta, Egypt, on October 11, 1946. He received the B.Sc. degree (with distinction) in Communications Engineering from Menoufia University, Egypt, in June 1969, the M.Sc. degree in Communication Engineering from Helwan University, Egypt, in April 1978, and the Ph.D. degree (very honorable) in Electronic Engineering from the National Polytechnic Institute, Toulouse, France, in June 1985. From September 1969 to July 1978, he was a Demonstrator. In July 1978, he was an Assistant Lecturer. In November 1985, he was a Lecturer. In February 1990, he was an Assistant Professor. In September 1995, he was named Professor in the Faculty of Electronic Engineering, Menoufia University, Communications Department. He was appointed as Vice Dean from February 2002 to October 2005, and Head of the Communications Department, from November 2005 to July 2007. At present, he is a Professor Emeritus at the same department. His main research interests are surface acoustic wave devices, optical devices, superconductor devices, medical applications of ultrasound, medical imaging, and bio-informatics.

Adel S. El-Fishawy received the B.Sc. in Electronics and Communications Engineering, Menoufia University, in 1974 and the M.Sc. degree from Cairo University, Egypt, in 1982. He received the Ph.D. degree in Signals and Systems from Drexel University, ECE Department, Philadelphia, PA, USA, 1990. He is working as a Professor Emeritus with the Department of Electronics and Electrical Communications Engineering, Faculty of Electronic Engineering, Menoufia University, Egypt. His areas of interest are electronics, modeling and simulation, digital communications, signal, speech, biomedical image processing, and digital communications.

S. El-Rabaie (SM'92) was born in Sires Elian, Egypt, in 1953. He received the B.Sc. degree (with honors) in Radio Communications from Tanta University, Tanta, Egypt, in 1976, the M.Sc. degree in Communication Systems from Menoufia University, Menouf, Egypt, in 1981, and the Ph.D. degree in Microwave Device Engineering from Queen's University of Belfast, Belfast, U.K., in 1986. In his Doctoral Research, he constructed a Computer-Aided Design (CAD) package used in nonlinear circuit simulations based on the harmonic balance techniques. Up to February 1989, he was a Postdoctoral Fellow with the Department of Electronic Engineering, Queen's University of Belfast. He was invited as a Research Fellow in the College of Engineering and Technology, Northern Arizona University, Flagstaff, in 1992 and as a Visiting Professor at Ecole Poly technique de Montreal, Montreal, QC, Canada, in 1994. He has authored and co-authored more than 300 papers and nineteen textbooks. He was given several awards (Salah Amer Award of Electronics in 1993, The Best Researcher on (CAD) from Menoufia University in 1995). He acts as a Reviewer and Member of the Editorial Board for several scientific journals. He has participated in translating the first part of the Arabic Encyclopedia. Professor El-Rabaie was the Head of the Electronics and Communication Engineering Department, Faculty of Electronic Engineering, Menoufia University, and after that the Vice Dean of Postgraduate Studies and Research at the same Faculty. Prof. El-Rabaie is involved now in different research areas including CAD of nonlinear

Turky Alotaiby received the B.Sc. degree in Computer Information Sciences from King Saud University, Saudi Arabia, in 1992, and the M.Sc. degree in Computer Information Systems and the Ph.D. degree in Computer Science from the Florida Institute of Technology, USA, in 1998 and in 2004, respectively. He spent three months (scientific trip) with the Montreal Neurological Institute, McGill University, Canada, in 2013. He is currently an Associate Research Professor with the National Center for Artificial Intelligence and Big Data Technology/Communication and Information Technology Institute, King AbdulAziz City for Science and Technology, Saudi Arabia. He has published several papers in conferences and refereed journals. His current research interests include physiological signals processing, pattern recognition, and time series modeling and prediction.

Saleh A. Alshebeili has over 25 years of teaching and research experience in the areas of Communications and Signal Processing. He was a Professor and the Chairman of the Electrical Engineering Department, King Saud University (2001–2005). He has been the Co-Founder and the Director of the Technology Innovation Center, RF, and Photonics for the e-Society (RFTONICS), since 2011, supported by the King Abdulaziz City for Science and Technology (KACST). He has also an active involvement in the review process of a number of research journals, KACST general directorate grants programs, and national and international symposiums and conferences. He is a member of the Board of Directors of the King Abdullah Institute for Research and Consulting Studies (2007–2009), the Board of Directors of the Prince Sultan Advanced Technologies Research Institute (PSATRI) (2008–2017), the Managing Director of PSATRI (2008–2011), and the Director of the Saudi-Telecom Research Chair (2008–2012). He was on the Editorial Board of the International Journal of Engineering Science, King Saud University (2009–2012).

Fathi E. Abd El-Samie received the B.Sc. (Hons.), M.Sc., and Ph.D. degrees from Menoufia University, Menouf, Egypt, in 1998, 2001, and 2005, respectively. Since 2005, he has been a Teaching Staff Member with the Department of Electronics and Electrical Communications, Faculty of Electronic Engineering, Menoufia University. He worked as a Researcher at KACST-TIC in Radio Frequency and Photonics for the e-Society (RFTONICs) from 2013 to 2015. His current research interests include image processing, multimedia communications, medical signal and image processing, optical signal processing, and digital communications. He was a recipient of the Most Cited Paper Award from the Digital Signal Processing journal in 2008.

Authors and Affiliations

Heba M. Emara[1] · Mohamed Elwekeil[1] · Taha E. Taha[1] · Adel S. El-Fishawy[1] · El-Sayed M. El-Rabaie[1] · Turky Alotaiby[2] · Saleh A. Alshebeili[3] · Fathi E. Abd El-Samie[1,4]

Mohamed Elwekeil
mohamed.elwekeil@el-eng.menofia.edu.eg

Taha E. Taha
taha117@hotmail.com

Adel S. El-Fishawy
aelfishawy@hotmail.com

El-Sayed M. El-Rabaie
srabie1@yahoo.com

Turky Alotaiby
totaiby@kacst.edu.sa

Saleh A. Alshebeili
dsaleh@ksu.edu.sa

Fathi E. Abd El-Samie
fathi_sayed@yahoo.com

[1] Department of Electronics and Electrical Communications Engineering, Faculty of Electronic Engineering, Menoufia University, Menouf 32952, Egypt

[2] KACST, Riyadh, Kingdom of Saudi Arabia

[3] Electrical Engineering Department, KACST-TIC in Radio Frequency and Photonics for the e-Society (RFTONICS), King Saud University, Riyadh, Kingdom of Saudi Arabia

[4] Department of Information Technology, College of Computer and Information Sciences, Princess Nourah bint Abdulrahman University, Riyadh 84428, Kingdom of Saudi Arabia